Published in final edited form as:
Protein Expr Purif. 2008 February ; 57(2): 271–279.

Expression, purification, and characterization of a structurally disordered and functional C-terminal autoinhibitory domain (AID) of the 70 kDa 40S ribosomal protein S6 kinase-1 (S6K1)

Timothy J. Ragan[a,c], **Duncan B. Ross**[a,c], **Malik M. Keshwani**[b], and **Thomas K. Harris**[a,*]

a*Department of Biochemistry and Molecular Biology, University of Miami School of Medicine, P. O. Box 016129, Miami, FL 33101-6129*

b*Department of Chemistry, University of Miami, P. O. Box 249118, Coral Gables, FL 33124-0431*

Abstract

S6K1 is a member of the AGC subfamily of serine-threonine protein kinases, whereby catalytic activation requires dual phosphorylation of critical residues in the conserved T-loop (T229) and hydrophobic motif (HM; T389) peptide regions of its catalytic kinase domain (residues 1-398). In addition to its kinase domain, S6K1 contains a C-terminal autoinhibitory domain (AID; residues 399-502), which prevents T-loop and HM phosphorylation; and autoinhibition is relieved on multi-site Ser-Thr phosphorylation of the AID (S411, S418, T421, and S424). Interestingly, 66 of the 104 C-terminal AID amino acid residues were computer predicted to exist in structurally disordered peptide regions, begetting interest as to how such dynamics could be coupled to autoregulation. To begin addressing this issue, we developed and optimized protocols for efficient AID expression and purification. Consistent with computer predictions, aberrant mobilities in both SDS-PAGE and size-exclusion chromatography, as well as low chemical shift dispersion in ^{1}H-^{15}N HSQC NMR spectra, indicated purified recombinant AID to be largely unfolded. Yet, trans-addition of purified AID effectively inhibited PDK1-catalyzed T-loop phosphorylation of a catalytic kinase domain construct of S6K1. Using an identical purification protocol, similar protein yields of a tetraphospho-mimic mutant AID(D_2ED) construct were obtained; and this construct displayed only weak inhibition of PDK1-catalyzed T229 phosphorylation. Purification of the structurally 'disordered' and functional C-terminal AID and AID(D_2ED) constructs will facilitate studies aimed to understand the role of conformational plasticity and protein phosphorylation in modulating autoregulatory domain-domain interactions.

Keywords

custom gene synthesis; intrinsic disorder; disordered proteins; autoinhibition; phosphoinositide-dependent protein kinase-1; PDK1; proteolysis inhibition; minimal media

*To whom correspondence should be addressed: T.K.H.: Tel: 305-243-3358; Fax: 305-243-3955; and E-mail: tkharris@miami.edu
[c]These authors contributed equally to this work.

Introduction

A key requirement for higher eukaryotic cells in sustaining prolific capacity is growth regulation, whereby increasing cellular mass and size prerequisite to division derives from coordinate macromolecular biosynthesis. The 70-kDa 40S ribosomal protein S6 kinase-1 (S6K1)[1] is a key enzyme in coordinating cell growth with proliferation, as *mitogen*, *nutrient*, and *energy status* signaling pathways converge to activate S6K1 and initiate protein translation [1-5]. Two S6K1 isoforms (**Accession No. NM003161**; αI and αII isoforms) are produced from a single gene by alternative mRNA splicing and the use of an alternative translational start site [6]. The 525 residue αI isoform contains an N-terminal 23 residue segment that encodes a polybasic nuclear localization motif; whereas the cytoplasmic αII isoform starts at a Met residue equivalent to Met24 in the αI isoform, and the sequences of both isoforms are identical thereafter.

S6K1 is a member of the AGC subfamily of serine-threonine protein kinases in which amino acid sequences are conserved in a segment of the catalytic kinase domain known as the activation loop or T-loop, as well as in a segment near the C-terminus of the kinase domain known as the hydrophobic motif (HM) [7]. Similar to other AGC kinase family members, catalytic activation of S6K1 requires dual phosphorylation of a critical residue in both the T-loop and HM. For the full length S6K1αI isoform these residues correspond to T252 and T412, respectively [8]; whereas in the S6K1αII isoform the identical residues correspond to T229 and T389 [9]. In a PI3K-dependent manner, mTOR phosphorylates the HM residue of S6K1 which serves to recruit and activate the upstream T-loop kinase, PDK1 [1-5]. With combined knowledge from available amino acid sequence alignments and X-ray structures, molecular modeling and biochemical testing now provide strong evidence for a common AGC kinase activation mechanism in which the phosphorylated HM interacts with a phosphate binding pocket located in the small N-lobe of the kinase [10]. This intramolecular interaction acts

[1]*Abbreviations used*:

AID autoinhibitory domain

GST glutathione S-transferase

His_6-S6K1αII(ΔAID)-T389E catalytic kinase domain construct of S6K1 αII isoform (residues 1-397) with N-terminal His_6 affinity tag

His_6-PDK1(ΔPH) catalytic kinase domain construct of PDK1 (residues 51-359) with N-terminal His_6 affinity tag

HM hydrophobic motif

HSQC heteronuclear single quantum coherence

IPTG isopropyl-*β*-D-thiogalactopyranoside

λPP Lambda protein phosphatase

PDK1 phosphoinositide-dependent protein kinase-1

PH pleckstrin homology domain

S6K1 70-kDa 40S ribosomal protein S6 kinase-1.

synergistically with T-loop phosphorylation to stabilize the active conformation, whereby a critical Glu residue in the αC-helix forms an ion pair with the catalytic Lys that functions to position the terminal phosphate of ATP for phosphotransfer in the kinase reaction.

The most distinguishing characteristic of S6K1 is its C-terminal autoinhibitory domain (AID), which suppresses catalytic activation by blocking the upstream kinase-mediated T-loop and HM phosphorylation events [8,9]. On the basis of structure-function mutagenesis studies, a model has been proposed whereby an autoinhibitory conformation is stabilized by electrostatic interactions between acidic residues of the N-terminal kinase domain and basic residues of the C-terminal AID; and multi-site Ser-Thr phosphorylation of AID (Fig. 1A; S411, S418, T421, and S424 in S6K1αII) destabilizes such an autoinhibitory domain-domain interaction [11-14]. Although no conclusive evidence has been obtained confirming the identity of the AID kinases, all of these Ser-Thr sites precede a proline residue and reside in a consensus motif similar to those known to serve as recognition determinants for MAP kinases such as ERK [15]. Indubitably, as these sites exhibited increased phosphorylation upon mitogen treatment [11,12] together with the observation that ERK was shown to phosphorylate S6K1αII in vitro [16], it has been reasoned that the RAS/MAPK pathway controls the initial or priming phosphorylations in the AID of S6K1αII [17,18]. Most interestingly, the AID exhibits no strong sequence homology to the non-redundant (nr) NCBI database yielding little insight to possible protein folds that may account for its evolutionary selection.

In this paper, we report PCR-based gene synthesis, *E. coli* expression, purification, and characterization of the C-terminal AID construct of S6K1 (Fig. 1A). Consistent with computer predictions of a high degree of AID structural disorder, a ^{1}H-^{15}N HSQC NMR spectrum indicated that purified recombinant AID is largely unfolded. Nevertheless, purified AID was shown to effectively inhibit, *in trans*, PDK1-catalyzed T229 phosphorylation of a Lambda protein phosphatase (λPP)-treated form of the T389E mutant S6K1αII kinase construct. Using an identical purification protocol, similar protein yields of a tetraphospho-mimic mutant AID (D_2ED) construct (S411D, S418D, T421E, and S424D in S6K1αII) were obtained; and this construct displayed weak inhibition of PDK1-catalyzed T229 phosphorylation of λPP-treated S6K1αII-T389E. The observed difference in the abilities of AID and AID(D_2ED) to trans-inhibit S6K1 phosphorylation by PDK1 will facilitate detailed structural and kinetic studies aimed to understand mechanisms (i) by which a structurally disordered C-terminal AID functions to inhibit S6K1 catalytic activation and (ii) how AID phosphorylation diminishes such inhibition.

Materials and methods

Materials

The pGEX-6P-1 protein expression vector, GST-PreScission™ protease, ÄKTAbasic 100 (FPLC), Prepacked GSTrap HP columns (5 mL), and the Superdex™ 75 16/60 size-exclusion column were from GE Healthcare Biosciences (Piscataway, NJ). The BL21 (DE3) protein expression strain of *E. coli* was from Novagen (Madison, WI). The cOmplete™ Protease Inhibitor Cocktail Tablets were from Roche Applied Science (Indianapolis, IN). $^{15}NH_4Cl$ was from Cambridge Isotope Laboratories, Inc. (Andover, MA). The N-terminal His_6 affinity tagged kinase domains of (i) S6K1 containing the phospho-mimicking mutation in the HM (His_6-S6K1αII(ΔAID)-T389E; residues 1-398) and (ii) PDK1 (His_6-PDK1(ΔPH); residues 51-359) were expressed using the Bac-to-Bac® Baculovirus Expression System (Invitrogen Inc., Carlsbad, CA) and His_6 affinity purified exactly as described for full length His_6-PDK1 [19]. All other chemicals, salts, and buffers were from Sigma, Inc. (St. Louis, MO). For preparation of ^{15}N-isotopic labeled AID, chromatographic and sample buffers were treated with Chelex, which was from Bio-Rad Laboratories (Hercules, CA).

Prediction of AID disorder

The amino acid sequence of the C-terminal AID of S6K1 (residues 399-502 in S6K1αII) was analyzed for relative amounts of disordered and ordered peptide regions by the PONDR® VL-XT software (Molecular Kinetics, Inc.). PONDR® (predictor of natural disordered regions) is a set of neural network predictors, which utilizes local amino acid composition, flexibility, hydropathy, coordination number, and other factors to score and classify each residue within a sequence as either disordered or ordered. PONDR® VL-XT integrates three feed forward neural networks: the variously characterized long, version 1 (VL1) predictor [20], which predicts non-terminal residues, and the X-ray characterized N- and C-terminal predictors (XT) [21], which predicts terminal residues. Output for the VL1 predictor starts and ends 11 amino acids from the termini. The XT predictors output provides predictions up to 14 amino acids from their respective ends. A simple average is taken for the overlapping predictions; and a sliding window of nine amino acids is used to smooth the prediction values along the length of the sequence. Unsmoothed prediction values from the XT predictors are used for the first and last four sequence positions.

Expression and purification of AID

The TBIO method of primer design and PCR-based gene synthesis [22] was used to assemble cDNA fragments encoding the C-terminal AID of S6K1 (residues 422-525 in αI or residues 399-502 in αII) (Supplemental Material). A sequence-verified *BamH*I-*Xho*I fragment containing the AID construct (Fig. 1A) was doubly digested from the pCR®-Blunt II-TOPO® plasmid vector and directionally ligated into the pGEX-6P-1 protein expression vector, which provided an N-terminal GST affinity tag with a GST-PreScission™ protease cleavage site (Fig. 1B). The protein expression vector was transformed into the BL21 (DE3) protein expression strain of *E. coli*.

PG minimal medium [23] was prepared with the following modifications. First, a desired total volume of 50 mM Na_2HPO_4, 50 mM KH_2PO_4, and 5 mM Na_2SO_4 was mixed and 500-mL aliquots were placed into 2-L baffled-bottom flasks, which were subjected to autoclave sterilization. Immediately before inoculation with starter culture, final concentrations of 2 mM $MgSO_4$, 56 mM NH_4Cl (1.5 g), 0.4% glucose (2 g), 100 μg/mL carbenicillin antibiotic, and 0.2× of a trace metal mixture were added to each 500 mL containing growth flask. A 1000× stock trace metal mixture in 60 mM HCl was prepared as described [23] and contained 50 mM $FeCl_3$, 20 mM $CaCl_2$, 10 mM $MnCl_2$-$4H_2O$, 10 mM $ZnSO_4$-$7H_2O$, and 2 mM each of $CoCl_2$-$6H_2O$, $CuCl_2$-$2H_2O$, $NiCl_2$-$6H_2O$, Na_2MoO_4-$2H_2O$, Na_2SeO_3, and H_3BO_3. A single colony raised from an LB/carbenicillin agar plate was used to inoculate a starter culture of 100 mL PG medium. After growing overnight at 37 °C, 15 mL of starter culture was used to inoculate each 500 mL growth flask, which was then allowed to grow at 37 °C to an optical cell density of 0.8 OD_{600}. For ^{15}N-isotopic labeling of AID, NH_4Cl was replaced with an identical amount of $^{15}NH_4Cl$.

Protein expression was induced by addition of 0.5 mM isopropyl-*β*-D-thiogalactopyranoside (IPTG) to cell cultures and allowed to proceed for 3 h at 37 °C. The cells (~3 grams per 500 mL of culture) were harvested by centrifugation for 10 min at 10000*g* in an SLA-3000 rotor (Sorvall); and 4 mL/(g cells) of cell wash buffer (50 mM phosphate buffer, pH 7.3, and 100 mM NaCl) was used to re-suspend, wash, and collect by centrifugation a single cell pellet, which was stored at -80 °C. The frozen cell pellet was thawed and re-suspended in 5 mL of cell lysis buffer (per gram of cell pellet) containing 50 mM phosphate buffer, pH 7.3, 100 mM NaCl, 1 mM dithiothreitol, 0.1% Triton X-100, 100 μg/mL N-*p*-tosyl-L-phenylalanine chloromethyl ketone (TPCK), 100 μg/mL N_α-tosyl-L-lysine chloromethyl ketone (TLCK), and cOmplete™ Protease Inhibitor Cocktail (1 tablet per 50 mL). The cells were lysed using the

EmulsiFlex-C3 high pressure homogenizer (Avestin, Inc.), and particulates were removed from the lysate by centrifugation for 20 min at 35,000*g* in an SS-34 rotor (Sorvall).

The soluble lysate, containing the GST-AID fusion construct was directly loaded by FPLC (0.1 mL/min) onto a 5 mL GSTrap FF affinity column equilibrated at 4 °C in 50 mM phosphate buffer, pH 7.3, 100 mM NaCl, and 0.1% Triton X-100. The column was subsequently washed (2 mL/min) until the absorbances at 280 nm returned to baseline. GST-AID was eluted with the same buffer but including 20 mM glutathione and pH 8.0. Fractions containing the GST-AID construct were combined and concentrated to ~0.5 mL using an Amicon ultrafiltration concentrators (5 kDa molecular weight cutoff). The GST affinity tag was cleaved by direct addition of GST-PreScission™ protease (2 μL of protease per mg of fusion construct), incubating at 4 °C for 16 h. The cleavage reaction was directly loaded by FPLC (1 mL/min) onto a Superdex™ 75 16/60 size-exclusion column equilibrated at 4 °C in 10 mM phosphate buffer, pH 7.3, and 100 mM NaCl. AID was resolved from all other protein components, detergents, and salts by isocratic elution with this buffer at 1 mL/min. Fractions containing cleaved recombinant AID in this buffer were combined and stored at -80 °C. AID protein concentrations were measured using a protein extinction coefficient $\varepsilon_{280\ nm}$ of 9900 M^{-1} cm^{-1}, as determined by the method of Gill and von Hippel [24].

NMR analysis of AID

For NMR analysis, 50 μM ^{15}N-isotopic labeled AID was prepared in 10 mM phosphate, pH 7.3, 100 mM NaCl, and 5% D_2O. Two-dimensional ^{1}H-^{15}N HSQC spectra were collected at 25 °C with a Bruker DMX500 NMR spectrometer (500 MHz for protons) equipped with pulsed-field gradients, four frequency channels, and a triple resonance cryoprobe with an actively shielded *z*-gradient. For the ^{1}H-^{15}N HSQC experiment, the data were recorded by using a pulse sequence in which the HSQC detection scheme was optimized to avoid water saturation [25] and by using the States-TPPI method [26] in the indirect dimension, with a relaxation delay of 1 s. The data were obtained with spectral widths of 1600 and 8000 Hz in f_1 (^{15}N) and f_2 (^{1}H), respectively, and with 256 and 1024 complex points, respectively in the t_1 and t_2 dimensions. A total of 16 transients were acquired for each hypercomplex t_1 point with ^{1}H and ^{15}N carriers positioned at 4.71 and 120 ppm, respectively. The final data matrix was 512 × 512 real points for the f_1 (^{15}N) and f_2 (^{1}H) dimensions, respectively. The program NMRPipe [27] was used to process the data. Proton chemical shifts are given with respect to the HDO signal taken to be 4.71 ppm relative to external TSP (0.0 ppm) at 25 °C. The ^{15}N chemical shifts were indirectly referenced.

AID inhibition of PDK1-catalyzed T229 phosphorylation of λPP-treated His_6-S6K1αII(ΔAID)-T389E

Baculovirus-mediated expression and His_6 affinity purification of the N-terminal His_6 affinity tagged kinase domain of S6K1 containing the phospho-mimicking mutation in the HM (His_6-S6K1αII(ΔAID)-T389E; residues 1-398) yielded a partially active kinase, as Western analysis detected a small amount of endogenous T229 phosphorylation. In order to dephosphorylate, 12 μM of purified His_6-S6K1αII(ΔAID)-T389E was incubated for 30 min at 25 °C with 2.5 units of λPP in 50 μL of λPP reaction buffer containing 50 mM Tris-HCl, pH 7.5, 0.1 mM EDTA, 5 mM dithiothreitol, 0.01% Brij 35, and 2 mM $MnCl_2$. PDK1-catalyzed trans-phosphorylation of T229 of λPP-treated His_6-S6K1αII(ΔAID)-T389E was performed at 25 °C in 50 mM Tris-HCl buffer, pH 7.5, containing 0.1% 2-mercaptoethanol, 10 mM $MgCl_2$, 0.1 mM sodium orthovanadate, 100 μM ATP, 1 μM λPP-treated His_6-S6K1αII(ΔAID)-T389E, 20 nM of purified active His_6-PDK1(ΔPH), and either AID (0 and 5 μM) or AID(D_2ED) (0, 5, 20 μM). The assays were initiated by addition of His_6-PDK1(ΔPH). At different times (5, 15, and 30 min), 5 μL of the reaction mixture was removed and quenched by addition of 5 μL of 2× SDS sample buffer; and 8.5 μL of each quenched reaction mixture (0.2 μg His_6-S6K1αII

(ΔAID)-T389E) was analyzed by SDS-PAGE and Western analysis for detection of T229 phosphorylation in His_6-S6K1αII(ΔAID)-T389E. Control assays (30 min) were carried out in which the His_6-PDK1(ΔPH) enzyme was omitted; and this quenched reaction mixture was analyzed and designated as time zero.

SDS-PAGE and Western analysis

Protein samples in SDS sample buffer were heated at 95 °C for 5 min and cooled on ice. All analytical SDS-PAGE were performed on 4-12% gradient Bis-Tris polyacrylamide gels (NuPage), which were developed at 150 V (constant) for ~1 h or until the tracking dye reached the bottom of the slab. For Western analysis of T229 phosphorylation in His_6-S6K1αII(ΔAID)-T389E (0.2 μg), proteins were transferred from the gel to Nitrocellulose Membrane Filter Paper Sandwich (Invitrogen) in a semidry blotting apparatus using Towbin buffer (25 mM Tris base, pH 8.3, 0.19 M glycine, and 20% methanol) as transferring solution. The resulting membranes were probed with the phospho-S6K1 (Thr229) polyclonal rabbit antibody according to the manufacturer's instructions (Novus Biologicals). Detection of immuno-protein complexes was carried out using secondary anti-rabbit antibody conjugated to horseradish peroxidase (HRP) (Cell Signaling Technology, Inc.) and Super Signal West Pico Luminal/Enhancer Solution and peroxide (Pierce).

Results and discussion

Prediction of AID disorder

Since amino acid sequence analysis of the C-terminal AID of S6K1 (Fig. 1A) revealed no strong sequence homology with protein sequences of known structure or function, we subjected the AID sequence to computer analysis using the PONDR® VL-XT software, which utilizes a set of neural network predictors to calculate the probability that amino acid residues exist in either structurally *ordered* or *disordered* peptide regions (Fig. 1C) [20]. In this analysis, *ordered* peptide regions are defined as having backbone atoms of each residue undergoing small-amplitude, thermally driven motions about equilibrium positions determined as time-averaged values; whereas *disordered* peptide regions exist as dynamic ensembles in which the atom positions of residing residues vary significantly over time with no specific equilibrium values [28]. The output of such analysis yields real numbers between one and zero for each amino acid residue, where one is the ideal prediction of disorder and zero is the ideal prediction of order. Outputs are typically not ideal and a threshold is applied with disorder assigned to values greater than or equal to 0.5. As displayed in Fig. 1C, 66 of 104 AID residues (63%) are predicted to be disordered and are located primarily in two long peptide regions spanning residues 401-418 and 443-488 (numbered according to S6K1αII). It is interesting to note that the regulatory S411, S418, T421, and S424 sites of phosphorylation reside in a short peptide region that transitions between the predicted disordered (residues 424-441) and ordered segments (residues 442-465). The number of intrinsically disordered proteins known to be involved in cell signaling and regulation is growing rapidly, and recent studies reveal that they are often involved in molecular recognition and protein modifications including phosphorylation [28-36].

Expression and purification of AID

In order to facilitate detailed biophysical studies aimed to understand mechanisms by which the C-terminal AID of S6K1 regulates its catalytic activation, we developed and optimized protocols for efficient AID expression and purification. First, a *BamH*I-*Xho*I fragment containing the C-terminal AID of S6K1 was efficiently synthesized in one PCR step using the TBIO method of primer design and gene assembly (Fig. 1A) [22]. For protein expression in *E. coli*, this construct was cloned into pGEX-6P-1, which provided an N-terminal GST affinity tag with a GST-PreScission™ protease cleavage site (Fig. 1B). Utilization of this expression

vector was advantageous on two accounts. Most importantly, the long GST-PreScission™ Protease cleavage recognition sequence (LEVLFQGP) renders it highly specific, as we found AID to be susceptible to nonspecific proteolysis when trying to remove affinity tags provided in other expression vectors that utilize serine protease recognition sequences (e.g., Factor Xa and thrombin). In addition, overall higher yields of affinity tagged constructs were best obtained when the AID was fused at the N-terminus with GST compared with N- and C-terminal fusions with either His_6 or thioredoxin. Next, expression of the recombinant GST-AID fusion construct was optimized in a slightly modified PG minimal medium [23], which enabled isotopic labeling for NMR spectroscopic characterization. In this medium, the BL21 (DE3) protein expression strain of *E. coli* provided GST-AID yields ~2-fold higher than with the Rosetta (DE3) and ~50-fold higher than with the HMS174 (DE3) expression strains. It is important to point out that expression of the recombinant GST-AID fusion construct *in LB medium* resulted in significantly lower overall recombinant protein yields.

The optimal yield of GST-AID, expressed in BL21 (DE3) *E. coli* grown in PG minimal medium, was achieved by inducing cell cultures (OD of 0.8) with 0.5 mM IPTG for 3 h at 37 °C. Cell lysate was collected by homogenization, and GST affinity purification typically yielded 17 ± 2 mg of total soluble protein from 1 L of culture medium (Table 1). Fig. 2A (lane 3) shows a number of protein species that co-eluted with the GST-AID construct, namely one high molecular weight contaminant (M_r = 70 kDa; likely Hsp70 chaperone) and a series of protein species with relative mobilities ranging between those of the full length GST-AID (M_r = 38 kDa) and GST alone (M_r = 23 kDa). Western analysis with anti-GST antibody confirmed the presence of GST in all of the latter species, indicating that the AID is highly susceptible to proteolysis. This “minimized” amount of proteolysis was achieved by including in the lysis buffer the irreversible serine protease inhibitors, TPCK and TLCK, in addition to use of the cOmplete™ Protease Inhibitor Cocktail (Roche). When both TPCK and TLCK were not included, AID proteolysis in the GST-AID construct was much more severe, greatly attenuating the yield of the full length GST-AID construct. The observed susceptibility to proteolysis, especially at the high number of different sites (Fig. 2A, lane 3), is consistent with the AID exhibiting a large degree of structural disorder [37].

Fig. 2A (lane 4) shows that GST-PreScission™ Protease efficiently cleaved the GST-AID fusion construct, yielding the full length GST affinity tag and full length AID. In this case, full length AID includes the additional N-terminal GPLGS residues as a result of using the pGEX-6P-1 expression vector (Fig. 1B). Due to their small sizes, the proteolyzed AID peptides were not detected in this SDS-PAGE. Nevertheless, Fig. 2B shows resolution of all protein species by Superdex™ 75 size exclusion chromatography, whereby the high molecular weight contaminant precedes cleaved GST, which is followed by a high yield of full length AID and a series of proteolyzed smaller fragments of the AID. The initial absorbance peak corresponds to Triton X-100, which was included in the purification buffer to reduce nonspecific binding of protein to the GST affinity column. Fig. 2A (lane 5) shows that this protocol efficiently yielded 2.0 ± 0.2 mg of purified full length AID from 1 L of culture medium (Table 1), which was judged by Coomassie blue staining of 4-12% SDS-PAGE to be of ≥95% homogeneity. For accurate determination of AID protein concentrations, it was necessary to utilize the method of Gill and von Hippel [24], which yielded a protein extinction coefficient $\varepsilon_{280\ nm}$ of 9900 M^{-1} cm^{-1}. When using colorimetric protein-Coomassie dye binding assays [38], AID concentrations were overestimated by ~50%, likely due to the highly basic nature of the AID construct (pI = 10.1).

Interestingly, AID displayed anomalously faster mobility in Superdex™ 75 size exclusion chromatography (apparent molecular mass of 15 kDa), as well as anomalously slower mobility in SDS-PAGE (apparent molecular mass of 15 kDa), which are 1.25-fold higher than the molecular mass of 11,988 Da calculated from its amino acid sequence (Figs. 1A and 1B,

S6K1αII residues 399-502 with N-terminal GPLGS residues). MALDI-TOF analysis of the purified AID construct determined a molecular mass of 11,988.4 Da (21st Century Biochemicals, Inc.), which confirmed the observed anomalous mobilities of full length and unmodified AID. Aberrant faster mobilities of *intrinsically disordered* proteins are observed in size-exclusion chromatography, since extended conformations result in larger hydrodynamic dimensions [37]. In addition, it has been pointed out that due to their unique amino acid compositions, *intrinsically disordered* proteins bind less SDS than globular proteins and therefore show aberrant slower mobilities in SDS-PAGE [37].

NMR analysis of AID

In order to further assess the relative degree of structural disorder in AID, it was expressed and purified to contain uniform ^{15}N-isotopic labeling for two-dimensional ^{1}H-^{15}N HSQC NMR analysis, which correlates the ^{1}H and ^{15}N chemical shifts (δ) of directly bonded ^{1}H-^{15}N pairs (i.e., backbone and side chain amide groups). Multidimensional NMR experiments have the potential to yield residue-specific conformational information of macromolecules in solution, as the backbone amides in folded proteins typically display a broad distribution of nuclear chemical shifts, ranging between ~7.0-9.5 ppm for protons and between ~105-135 ppm for nitrogens. For *intrinsically disordered* proteins, the inherent flexibility of the polypeptide chain and the rapid interconversion between multiple conformations results in poor chemical shift dispersion of most resonances, especially of protons, which narrow to a range between ~8.0-8.5. Fig. 3 shows the ^{1}H-^{15}N HSQC spectrum of uniformly ^{15}N-labeled AID. In general, the majority of backbone amide proton resonances exhibited poor chemical shift dispersion (~7.8-8.6 ppm), indicating substantial regions of structural disorder. In addition, the majority of resonances were either broadened or missing, indicating interconversion between multiple conformations occurring within the “intermediate” spectroscopic timescale. Since the amide nitrogen present in the side chains of both glutamine and asparagine contains two bonded protons (-NH_2), this group yields a pair of resonances with the same ^{15}N chemical shift but different ^{1}H chemical shifts. Thus, pairs of resonances are observed in the upfield regions (Fig. 3, ^{15}Nδ ~ 113 ppm and ^{1}Hδ ~ 7.1 ppm and ~7.3 ppm), as expected for the -NH_2 group in the side chains of the three asparagines and three glutamines (Fig. 1A, N444, N479, N501, Q446, Q460, and Q477). In addition, a single resonance is observed in the downfield regions (Fig. 3, ^{15}Nδ = 129 ppm and ^{1}Hδ = 10.1 ppm), as expected for the NεH of the aromatic indole side chain of the single tryptophan (Fig. 1A, W434).

AID inhibition of PDK1-catalyzed T229 phosphorylation of λPP treated His_6-S6K1αII(ΔAID)-T389E

The best characterized function of the C-terminal AID is inhibition of upstream kinase-mediated HM (T389) and T-loop (T229) phosphorylation events, required for S6K1αII activation [8,9]. As the ^{1}H-^{15}N HSQC NMR spectrum (Fig. 3) clearly confirmed the large degree of AID structural disorder predicted by computer analysis using the PONDR® VL-XT software (Fig. 1C), it became of immediate interest to test whether purified recombinant AID can function, in trans, to inhibit phosphorylation of a recombinant catalytic domain construct of S6K1. While numerous in vivo studies indicate mTOR to be the upstream kinase for HM (T389) phosphorylation, an in vitro assay for this reaction is not readily practical. In contrast, both in vivo and in vitro assays have been established for monitoring T-loop (T229) phosphorylation by the upstream kinase, PDK1; albeit that T389 of S6K1αII is either phosphorylated or mutated to a negatively charged residue [8,9]. In order to generate a catalytic domain construct of S6K1αII that would serve as a suitable in vitro substrate for monitoring PDK1-catalyzed T229 phosphorylation (Fig. 4), the His_6-S6K1αII(ΔAID)-T389E mutant was expressed, purified, and treated with Lambda protein phosphatase (λPP).

Fig. 4A shows that incubation of 1 μM of λPP-treated His_6-S6K1αII(ΔAID)-T389E with 20 nM PDK1 resulted in rapid (≤5 min) and site-specific T229 trans-phosphorylation, as detected by Western analysis with phospho-S6K1 (T229) polyclonal rabbit antibody. When this reaction was carried out in the presence of 5 μM AID, no T229 phosphorylation could be detected for times up to 30 min (Fig. 4B), indicating that trans-addition of purified recombinant 'disordered' AID does indeed effectively inhibit S6K1 phosphorylation by PDK1. Since it is known that multi-site Ser-Thr phosphorylation of AID (Fig. 1A, S411, S418, T421, and S424 in S6K1αII) destabilizes its autoinhibitory interaction with the kinase domain of S6K1 [11-14], we PCR-synthesized, expressed and purified the tetraphospho-mimic (S411D, S418D, T421E, and S424D) mutant construct, AID(D_2ED), exactly as described for AID. Fig. 4C shows that 5 μM AID(D_2ED) sustained only partial inhibition of PDK1-catalyzed T229 phosphorylation, which was potentiated on increasing AID(D_2ED) to 20 μM, indicating that the phospho-mimicking mutations weakened the autoinhibitory AID-S6K1 domain-domain trans-interaction.

Summary

In summary, 66 of the 104 C-terminal AID amino acid residues were computer predicted to exist in structurally disordered peptide regions. Regions of intrinsic disorder are characterized by a distribution of Ramachandran phi and psi angles for each amino acid residue, giving rise to an ensemble of interconverting conformers; and flexible protein regions are known to be easy targets for proteolysis. Indeed, our initial attempts to express and purify AID were hindered by its high susceptibility to proteolysis. Optimal bacterial expression and affinity purification of full length AID was achieved by (i) fusing GST to the N-terminus, (ii) growing the BL21 (DE3) strain of *E. coli* in PG minimal medium, (iii) adding the irreversible protease inhibitors TPCK and TLCK to the lysis buffer, (iv) using the highly selective PreScission™ Protease to remove the GST affinity tag, and (v) using the Superdex™ 75 size-exclusion column to resolve cleaved full length AID from smaller proteolyzed fragments. In addition to its high susceptibility to proteolysis, purified recombinant AID (M_{calc} = 12 kDa) exhibited other characteristics typical to intrinsically disordered proteins including (i) anomalously slow mobility in SDS-PAGE (M_r = 15 kDa), (ii) anomalously fast mobility in size-exclusion chromatography (M_r = 15 kDa), and (iii) low chemical shift dispersion in ^1H-^{15}N HSQC NMR spectra. Most significantly, 5 μM AID effectively inhibited PDK1-catalyzed T229 phosphorylation in the T-loop of the S6K1 catalytic kinase domain construct, His_6-S6K1 (ΔAID)-T389E. In addition, a S411D-S418D-T421E-S424D mutant construct, AID(D_2ED), was PCR-synthesized and purified using identical protocols, and similar protein yields were obtained. Consistent with the proposed electrostatic model for regulation of S6K1 autoinhibition [11-14], the tetraphospho-mimicking mutations in the AID(D_2ED) construct significantly decreased AID-mediated inhibition of PDK1-catalytzed T229 phosphorylation of His_6-S6K1(ΔAID)-T389E.

Supplementary Material

Refer to Web version on PubMed Central for supplementary material.

Acknowledgements

This research was supported by a grant from the National Institute of General Medical Sciences (GM69868) to T.K.H. and a Maytag Graduate Fellowship to M.M.K..

References

1. Holz MK, Ballif BA, Gygi SP, Blenis J. mTOR and S6K1 mediate assembly of the translation preinitiation complex through dynamic protein interchange and ordered phosphorylation events. Cell 2006;123:569–580. [PubMed: 16286006]
2. Tee AR, Blenis J. mTOR, translational control and human disease. Semin. Cell Dev. Biol 2005;16:29–37. [PubMed: 15659337]
3. Fingar DC, Blenis J. Target of rapamycin (TOR): an integrator of nutrient and growth factor signals and coordinator of cell growth and cell cycle progression. Oncogene 2004;23:3151–3171. [PubMed: 15094765]
4. Richardson CJ, Schalm SS, Blenis J. PI3-kinase and TOR: PIKTORing cell growth. Semin. Cell Dev. Biol 2004;15:147–159. [PubMed: 15209374]
5. Martin KA, Blenis J. Coordinate regulation of translation by the PI 3-kinase and mTOR pathways. Adv. Cancer Res 2002;86:1–39. [PubMed: 12374276]
6. Grove JR, Banerjee P, Balasubramanyam A, Coffer PJ, Price DJ, Avruch J, Woodgett JR. Cloning and expression of two human p70 S6 kinase polypeptides differing only at their amino termini. Mol. Cell Biol 1991;11:5541–5550. [PubMed: 1922062]
7. Peterson RT, Schreiber SL. Kinase phosphorylation: keeping it all in the family. Curr. Biol 1999;9:R521–R524. [PubMed: 10421571]
8. Alessi D, Kozlowski MT, Weng Q-P, Morrice N, Avruch J. 3-Phosphoinositide-dependent protein kinase 1 (PDK1) phosphorylates and activates the p70 S6 kinase in vivo and in vitro. Curr. Biol 1997;8:69–81. [PubMed: 9427642]
9. Pullen N, Dennis PB, Andjelkovic M, Dufner A, Kozma SC, Hemmings BA, Thomas G. Phosphorylation and activation of $p70^{s6k}$ by PDK1. Science 1998;279:707–710. [PubMed: 9445476]
10. Frödin M, Antal TL, Dümmler BA, Jensen CJ, Deak M, Gammeltoft S, Biondi RM. A phosphoserine/threonine-binding pocket in AGC kinases and PDK1 mediates activation by hydrophobic motif phosphorylation. EMBO J 2002;21:5396–5407. [PubMed: 12374740]
11. Cheatham L, Monfar M, Chou MM, Blenis J. Structural and functional analysis of p70 S6 kinase. Proc. Natl. Acad. Sci. USA 1995;92:11696–11700. [PubMed: 8524831]
12. Weng Q, Andrabi K, Kozlowski MT, Grove JR, Avruch J. Multiple independent inputs are required for activation of the p70 S6 kinase. Mol. Cell. Biol 1995;15:2333–2340. [PubMed: 7739516]
13. Dennis PB, Pullen N, Kozma SC, Thomas G. The principal rapamycin-sensitive p70(s6k) phosphorylation sites, T-229 and T-389, are differentially regulated by rapamycin-insensitive kinase kinases. Mol. Cell. Biol 1996;16:6242–6251. [PubMed: 8887654]
14. Pullen N, Thomas G. The modular phosphorylation and activation of p70s6k. FEBS Lett 1997;410:78–82. [PubMed: 9247127]
15. Ferrari S, Bannworth W, Morley SJ, Totty NF, Thomas G. Activation of p70S6K is associated with phosphorylation of four clustered sites displaying Ser/Thr-Pro motifs. Proc. Natl. Acad. Sci. USA 1992;89:7282–7285. [PubMed: 1496022]
16. Mukhopadhayay NK, Price DJ, Kyriakis JM, Pelech SL, Sanghera J, Avruch J. An array of insulin-activated, proline-directed serine/threonine protein kinases phosphorylate the p70 S6 kinase. J. Biol. Chem 1992;267:3325–3335. [PubMed: 1737788]
17. Dufner A, Thomas G. Ribosomal S6 kinase signaling and the control of translation. Exp. Cell Res 1999;253:100–109. [PubMed: 10579915]
18. Weng QP, Kozlowski M, Belham C, Zhang A, Comb MJ, Avruch J. Regulation of the p70 S6 kinase by phosphorylation in vivo. Analysis using site-specific anti-phosphopeptide antibodies. J. Biol. Chem 1998;273:16621–16629. [PubMed: 9632736]
19. Gao X, Yo P, Harris TK. Improved yields for baculovirus-mediated expression of human His_6-PDK1 and His_6-PKBβ/Akt2 and characterization of phospho-specific isoforms for design of inhibitors that stabilize inactive conformations. Protein Expr. Purif 2005;43:44–56. [PubMed: 16084396]
20. Romero P, Obradović Z, Li X, Garner EC, Brown CJ, Dunker AK. Sequence complexity of disordered proteins. Proteins: Struct. Funct. Genet 2001;42:38–48. [PubMed: 11093259]
21. Li X, Romero P, Rani M, Dunker AK. Predicting protein disorder for N-, C-, and internal regions. Genome Inform. Ser. Workshop Genome Inform 1999;10:30–40.

22. Gao X, Yo P, Keith A, Ragan TJ, Harris TK. Thermodynamically balanced inside-out (TBIO) PCR-based gene synthesis: a novel method of primer design for high fidelity assembly of longer gene sequences. Nuc. Acids Res 2003;31:e143.
23. Studier FW. Protein production by auto-induction in high density shaking cultures. Protein Expr. Purif 2005;41:207–234. [PubMed: 15915565]
24. Gill SC, von Hipple PH. Calculation of protein extinction coefficients from amino acid sequence data. Anal. Biochem 1989;182:319–326. [PubMed: 2610349]
25. Mori S, Abeygunawardana C, Johnson MO, van Zijl PCM. Improved sensitivity of HSQC spectra of exchanging protons at short interscan delays using a new fast HSQC (FHSQC) detection scheme that avoids water saturation. J. Magn. Reson 1995;108B:94–98.
26. Marion D, Driscoll PC, Kay LE, Wingfield PT, Bax A, Gronenborn AM, Clore GM. Overcoming the overlap problem in the assignment of ^{1}H NMR spectra of larger proteins by use of three-dimensional heteronuclear ^{1}H-^{15}N Hartmann-Hahn multiple quantum coherence spectroscopy: application to interleukin 1β. Biochemistry 1989;28:6150–6156. [PubMed: 2675964]
27. Delaglio F, Grzesiek S, Vuister GW, Zhu G, Pfiefer J, Bax A. NMRPipe: a multidimensional spectral processing system based on UNIX pipes. J. Biomol. NMR 1995;6:277–293. [PubMed: 8520220]
28. Radivojac P, Iakoucheva LM, Obradović CJ, Uversky VN, Oldfield AK, Dunker Z. Intrinsic disorder and functional proteomics. Biophys. J 2007;92:1439–1456. [PubMed: 17158572]
29. Vacic V, Oldfield CJ, Mohan A, Radivojac P, Cortese MS, Uversky VN, Dunker AK. Characterization of molecular recognition features, MoRFs, and their binding partners. J. Proteome Res 2007;6:2351–2366. [PubMed: 17488107]
30. Mohan A, Oldfield CJ, Radivojac P, Vacic V, Cortese MS, Dunker AK, Uversky VN. Analysis of molecular recognition features (MoRFs). J. Mol. Biol 2006;362:1043–1059. [PubMed: 16935303]
31. Uversky VN, Oldfield CJ, Dunker AK. Showing your ID: intrinsic disorder as an ID for recognition, regulation and cell signalling. J. Mol. Recognit 2005;18:343–384. [PubMed: 16094605]
32. Dunker AK, Cortese MS, Romero P, Iakoucheva LM, Uversky VN. The roles of intrinsic disorder in protein interaction networks. FEBS J 2005;272:5129–5148. [PubMed: 16218947]
33. Iakoucheva LM, Radivojac P, Brown CJ, O'Conner TR, Sikes JG, Obradović Z, Dunker AK. The importance of intrinsic disorder for protein phosphorylation. Nuc. Acids Res 2004;32:1037–1049.
34. Iakoucheva LM, Brown CJ, Lawson JD, Obradović Z, Dunker AK. Intrinsic disorder in cell-signaling and cancer-associated proteins. J. Mol. Biol 2002;323:573–584. [PubMed: 12381310]
35. Sickmeier M, Hamilton JA, LeGail T, Vacic V, Cortese MS, Tantos A, Szabo B, Tompa P, Chen J, Uversky VN, Obradović Z, Dunker AK. DisProt: the database of disordered proteins. Nuc. Acids Res 2007;35:D786–D793.
36. Vucetic S, Obradović Z, Vacic V, Radivojac P, Peng K, Iakoucheva LM, Cortese MS, Lawson JD, Brown CJ, Sikes JG, Newton CD, Dunker AK. DisProt: a database of protein disorder. Bioinformatics 2005;21:137–140. [PubMed: 15310560]
37. Receveur-Bréchot V, Bourhis J-M, Uversky VN, Canard B, Longhi S. Assessing protein disorder and induced folding. Proteins: Struct. Funct. Genet 2006;62:24–45. [PubMed: 16287116]
38. Bradford MM. A rapid and sensitive method for the quantitation of microgram quantities of protein utilizing the principle of protein-dye binding. Anal. Biochem 1976;72:248–254. [PubMed: 942051]

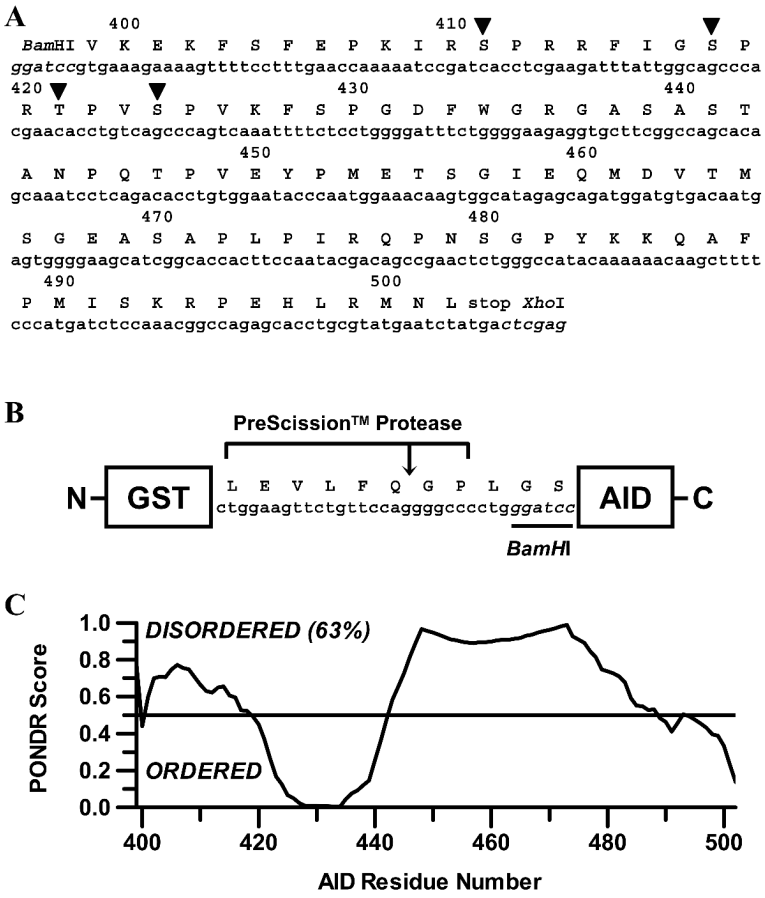

Fig. 1.

AID expression constructs and predicted regions of disorder. (A) Amino acid and DNA coding sequence of the C-terminal autoinhibitory domain of the 70 kDa 40S ribosomal protein S6 kinase-1 (AID; residues 399-502 in the S6K1αII isoform). This peptide region is highly basic with a calculated pI of 10.1. Italicized nucleotides at each terminus indicate restriction enzyme recognition sequences used to directionally ligate the protein coding region into the pGEX-6P-1 protein expression vector. The autoregulatory sites of Ser-Thr phosphorylation (S411, S418, T421, and S424) are indicated (▼). (B) Coding region of the recombinant pGEX-6P-1-AID expression vector depicting the recognition sequence and site of cleavage by the PreScission™ protease. (C) PONDR® VL-XT analysis. Amino acids with PONDR scores ≥0.5 are classified as being in 'disordered' peptide regions and those with scores <0.5 are classified as being in 'disordered' peptide regions.

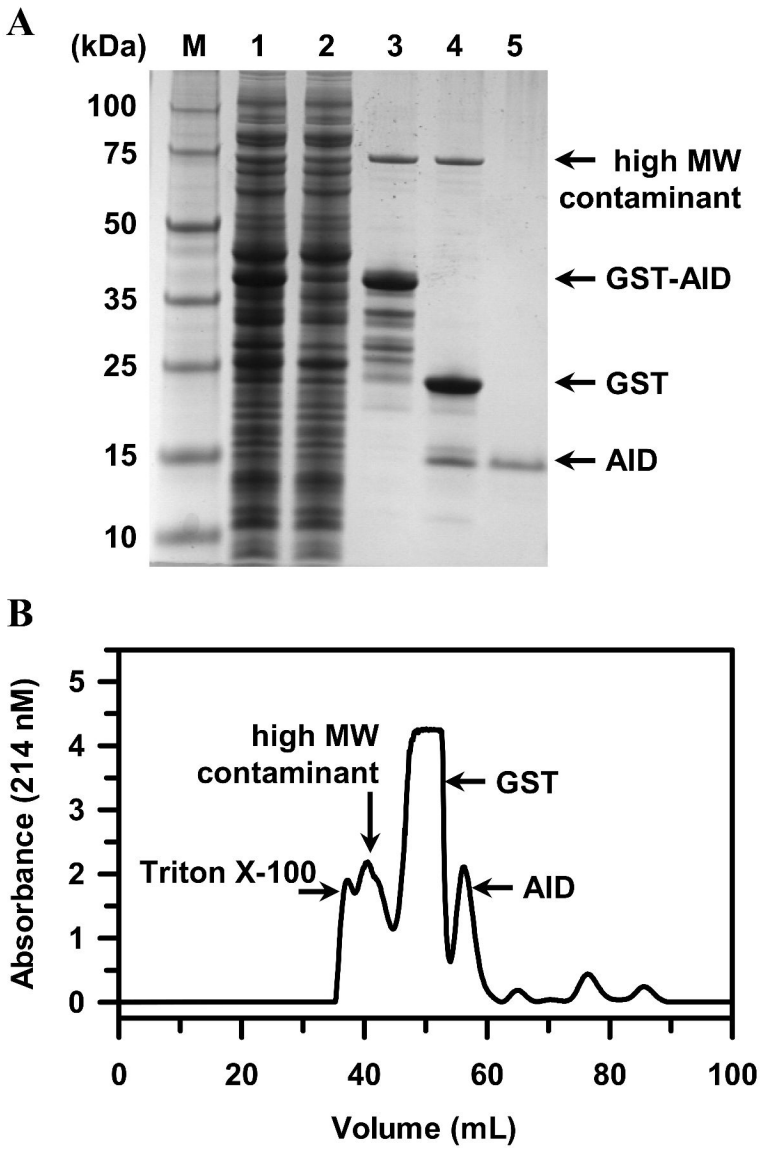

Fig. 2.

Purification of AID from *E. coli* lysate. (A) SDS-PAGE analysis with Coomassie staining. Lane 1 shows the total soluble lysate. Lane 2 shows the proteins from the soluble lysate that were not retained after passage over the GST Sepharose High Trap HP affinity column. Lane 3 shows the proteins that were retained and subsequently eluted from the GSTrap HP affinity column. Lane 4 shows the protein products obtained after digestion with GST-PreScission™ protease. Lane 5 shows purified AID resolved by Superdex™ 75 size-exclusion chromatography. (B) Superdex™ 75 size-exclusion purification of AID after digestion with GST-PreScission™ protease.

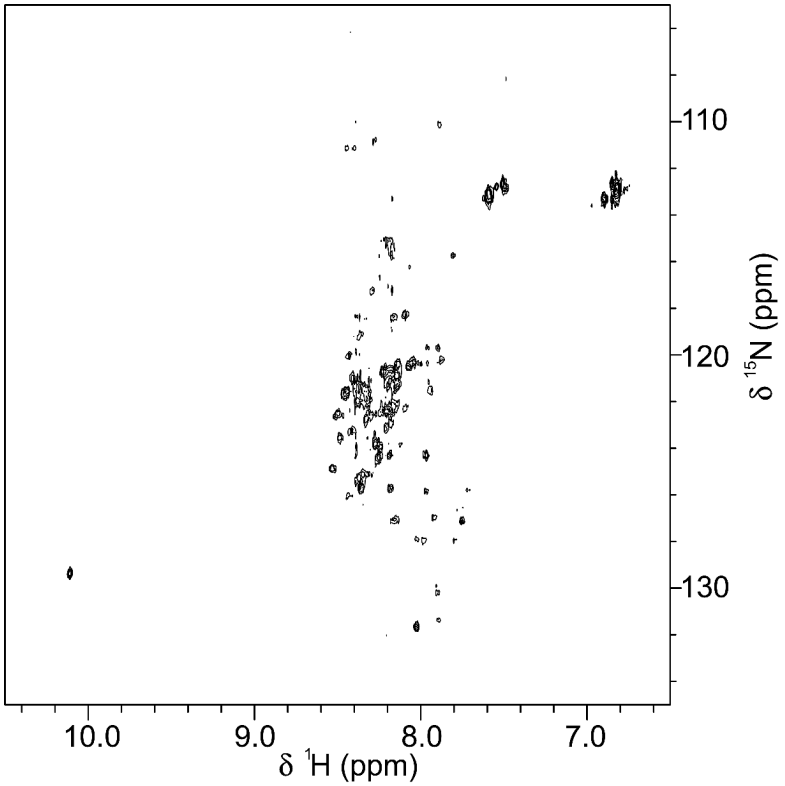

Fig. 3.

NMR analysis of AID. Two-dimensional ^{1}H-^{15}N HSQC spectrum of uniform ^{15}N-isotopic labeled AID. The final concentration of AID was 50 μM in 10 mM phosphate buffer, pH 7.3, containing 100 mM NaCl and 5% D_2O. Spectra were collected at 25 °C with a Bruker DMX500 NMR spectrometer (500 MHz for protons) equipped with a triple resonance cryoprobe.

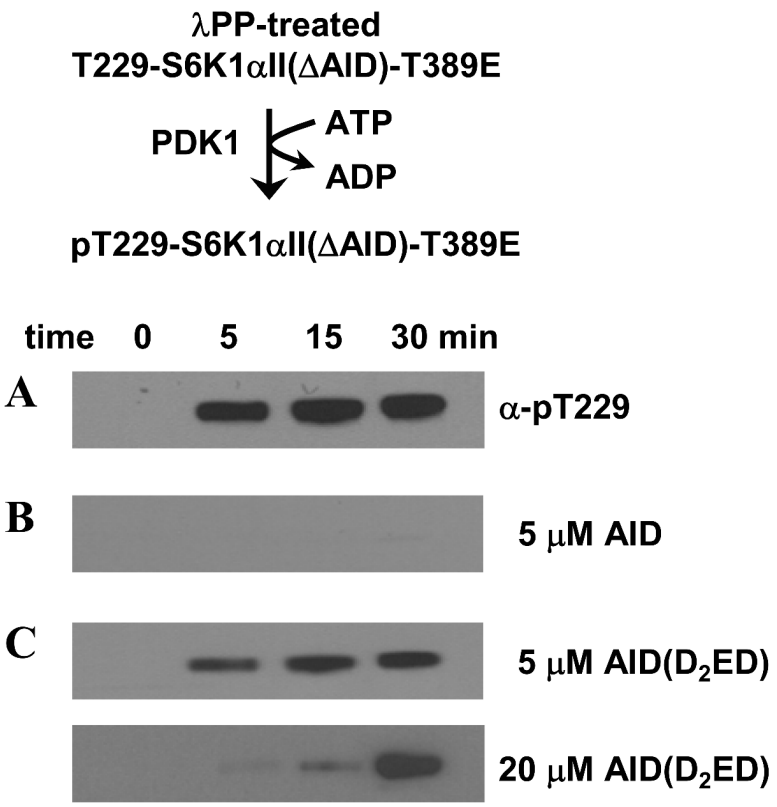

Fig. 4.

AID inhibition of PDK1-catalyzed T229 phosphorylation of λPP-treated His_6-S6K1αII (ΔAID)-T389E. Western analysis was used to follow the time dependence (0, 5, 15, and 30 min) for T229 phosphorylation that occurs on incubation of 1 μM λPP-treated His_6-S6K1αII (ΔAID)-T389E substrate with 20 nM PDK1 enzyme. Time dependences are shown for the (A) phosphorylation reaction alone; (B) the phosphorylation reaction in the presence of 5 μM AID; and (C) the phosphorylation reaction in the presence of either 5 μM or 20 μM AID(D_2ED).

Table 1

Purification of the C-terminal AID construct of S6K1 from *E. coli*[a]

Purification (Step)	Volume (mL)	Concentration (mg/mL)	Yield (mg)	Purification (fold)
Crude lysate	25	15 ± 2[b]	375 ± 50	N/A
GST affinity	10	1.7 ± 0.2[b]	17 ± 2	22
Superdex™ 75	5	0.40 ± 0.05[c]	2.0 ± 0.2	150

[a] All values are reported for purification from expression in 1 L of *E. coli*.

[b] Protein concentrations were measured by Bio-Rad protein assay.

[c] Purified AID concentrations were measured using $\varepsilon_{280\ nm}$ of 9900 M^{-1} cm^{-1} and converted to mg/mL using the calculated molecular mass of 11,988 Da.